CellPress

Cell Stem Cell
Article

Leptin-Receptor-Expressing Mesenchymal Stromal Cells Represent the Main Source of Bone Formed by Adult Bone Marrow

Bo O. Zhou,[1] Rui Yue,[1] Malea M. Murphy,[1] James G. Peyer,[1] and Sean J. Morrison[1,2,*]
[1]Children's Research Institute and Department of Pediatrics, University of Texas Southwestern Medical Center, Dallas, TX 75390, USA
[2]Howard Hughes Medical Institute
*Correspondence: sean.morrison@utsouthwestern.edu
http://dx.doi.org/10.1016/j.stem.2014.06.008

SUMMARY

Studies of the identity and physiological function of mesenchymal stromal cells (MSCs) have been hampered by a lack of markers that permit both prospective identification and fate mapping in vivo. We found that Leptin Receptor (LepR) is a marker that highly enriches bone marrow MSCs. Approximately 0.3% of bone marrow cells were LepR$^+$, 10% of which were CFU-Fs, accounting for 94% of bone marrow CFU-Fs. LepR$^+$ cells formed bone, cartilage, and adipocytes in culture and upon transplantation in vivo. LepR$^+$ cells were *Scf*-GFP$^+$, *Cxcl12*-DsRed^{high}, and *Nestin*-GFP^{low}, markers which also highly enriched CFU-Fs, but negative for *Nestin*-CreER and *NG2*-CreER, markers which were unlikely to be found in CFU-Fs. Fate-mapping showed that LepR$^+$ cells arose postnatally and gave rise to most bone and adipocytes formed in adult bone marrow, including bone regenerated after irradiation or fracture. LepR$^+$ cells were quiescent, but they proliferated after injury. Therefore, LepR$^+$ cells are the major source of bone and adipocytes in adult bone marrow.

INTRODUCTION

Multipotent mesenchymal stromal cells (MSCs) have been defined in culture as nonhematopoietic, plastic-adherent, colony-forming cells, referred to as colony-forming unit-fibroblasts (CFU-Fs), that can differentiate into osteogenic, chondrogenic, and adipogenic progeny (Bianco et al., 2008; Friedenstein et al., 1970; Horwitz et al., 2005; Pittenger et al., 1999). A fundamental question concerns the identity of the cells that form CFU-Fs in culture and their physiological function in vivo.

In vivo, MSCs are often perivascular (Crisan et al., 2008; Sacchetti et al., 2007). In human tissues, MSCs have been prospectively identified based on the lack of expression of endothelial and hematopoietic markers along with positive expression for CD146 (Sacchetti et al., 2007) or CD146 with platelet-derived growth factor receptor β (PDGFRβ), CD106, NG2, or some combination thereof (Chou et al., 2012; Crisan et al., 2008; Schwab and Gargett, 2007). CD146$^+$ MSCs from human bone marrow form osteogenic, chondrogenic, and adipogenic cells in culture and give rise to bone upon transplantation in vivo, forming bony ossicles that become invested with hematopoietic bone marrow (Sacchetti et al., 2007). The CD146$^+$ cells persist around sinusoidal blood vessels in the ossicles and express HSC niche factors. Ectopic bones that become invested with bone marrow can also be formed by CD105$^+$Thy1$^-$ mesenchymal cells from fetal mouse bones (Chan et al., 2009). Although much has been learned about the localization and developmental potential of MSCs, limitations in the ability to fate-map these cells in vivo have hindered our understanding of their normal physiological function.

Mouse MSCs have been prospectively identified based on the lack of expression of hematopoietic and endothelial markers and positive expression of PDGFRα (Morikawa et al., 2009; Omatsu et al., 2010; Park et al., 2012). The PDGFRα$^+$Sca-1$^+$CD45$^-$Ter119$^-$ subset of cells appears to reside primarily around arterioles but does not express the hematopoietic stem cell (HSC) niche factor *Cxcl12*, while PDGFRα$^+$Sca-1$^-$CD45$^-$Ter119$^-$ cells that express high levels of *Cxcl12*, also known as CXCL12-abundant reticular (CAR) cells, reside primarily around sinusoids (Morikawa et al., 2009; Omatsu et al., 2010). CAR cells include bipotent progenitors of osteoblasts and adipocytes (Omatsu et al., 2010). Ablation of CAR cells with diphtheria toxin (DT) depletes not only adipogenic and osteogenic progenitors, but also HSCs (Omatsu et al., 2010). These data suggest that MSCs within the bone marrow are a cellular component of the HSC niche.

Cells that express the *Nestin*-GFP transgene contain all of the CFU-Fs in mouse bone marrow (Kunisaki et al., 2013; Méndez-Ferrer et al., 2010). These cells also express high levels of the HSC niche factors *Cxcl12* and *Stem cell factor* (*Scf*) (Kunisaki et al., 2013; Méndez-Ferrer et al., 2010). *Nestin*-CreER-expressing cells in adult bone marrow can contribute to osteoblasts and chondrocytes, though no quantification was provided regarding their CFU-F content or their level of contribution to new bone (Méndez-Ferrer et al., 2010). *Nestin*-GFP is widely expressed by perivascular stromal cells in the bone marrow, but they express little endogenous *Nestin*, *Nestin*-CreER, or other *Nestin* transgenes (Ding et al., 2012). Furthermore, *Nestin*-GFP$^+$ cells are heterogeneous, including both *Nestin*-GFP^{high} cells that localize mainly around arterioles and *Nestin*-GFP^{low} cells that localize mainly around sinusoids, raising questions about the distribution of HSC niche factors and MSCs among these cell populations (Kunisaki et al., 2013).

During fetal development, Osterix (Osx) is expressed by cells that form bone marrow stroma, including perivascular, osteogenic, and adipogenic cells (Liu et al., 2013; Maes et al., 2010). In adult bone marrow, Osx is expressed by a subset of CAR cells (Omatsu et al., 2010), and fate mapping of these cells using *Osx*-CreER revealed a transient contribution to osteoblasts (Park et al., 2012). In contrast, *Mx-1*-Cre recombined widely among hematopoietic cells, PDGFRα$^+$ stromal cells, and CFU-Fs in the bone marrow, and these cells gave rise to most of the osteoblasts formed in adult bone marrow (Park et al., 2012). The widespread marking of both hematopoietic and stromal cells by *Mx-1*-Cre meant that this marker could not be used to prospectively identify osteogenic progenitors.

Recently, we identified Leptin Receptor$^+$ (LepR$^+$) perivascular stromal cells that are the major source of *Scf* and *Cxcl12* in the bone marrow (Ding and Morrison, 2013; Ding et al., 2012). Conditional deletion of *Scf* with *Lepr*-Cre led to the depletion of quiescent HSCs (Ding et al., 2012; Oguro et al., 2013) and conditional deletion of *Cxcl12* with *Lepr*-Cre led to HSC mobilization (Ding and Morrison, 2013). Here we show that LepR$^+$ cells are highly enriched for CFU-F and uniformly express *Prx1*-Cre, PDGFRα, and CD51, markers expressed by bone marrow MSCs. LepR$^+$ cells were the main source of new osteoblasts and adipocytes in adult bone marrow and could form bony ossicles that support hematopoiesis in vivo. In contrast, *Wnt1*-Cre-expressing neural-crest-derived cells and *Nestin*-CreER-expressing cells included few CFU-Fs and made little contribution to adult osteogenesis.

RESULTS

LepR$^+$ Bone Marrow Stromal Cells Are Around Sinusoids and Arterioles

Sections from wild-type mice exhibited perivascular LepR staining throughout the bone marrow, around both sinusoids and arterioles (Figures 1A, 1C, and 1D). The staining was in perivascular stromal cells that expressed the HSC niche factor *Scf* (Figure 1C). An antibody against the LepR extracellular domain stained in a pattern very similar to that of Tomato expression in *Lepr-cre; tdTomato* conditional reporter mice (Figure 1D). *Ubc-creER; Lepr$^{fl/fl}$* mice that had been treated with tamoxifen for 1 month to conditionally delete *Lepr* had little staining with the antibody in sections (Figure 1B) or in PDGFRα$^+$ CD45$^-$Ter119$^-$CD31$^-$ bone marrow stromal cells analyzed by flow cytometry (Figure S1A available online).

We identified sinusoids and arterioles based on VE-Cadherin (VE-Cad) staining, which bound endothelial cells in both sinusoids and arterioles, and SM22 staining, which specifically marked vascular smooth muscle around arterioles. Sinusoids were typically larger in diameter, less uniform, and thinner walled as compared to arterioles (Figure 1E). We observed LepR$^+$ cells around both sinusoids and arterioles throughout the bone marrow, though LepR$^+$ cells were much more prominent around some arterioles than others (Figure 1E). Nearly all the perisinusoidal LepR$^+$ cells were *Scf*-GFP$^+$; however, the periarteriolar LepR$^+$ cells, especially those densely surrounding larger arterioles, expressed less *Scf*-GFP (Figure 1E). The LepR$^+$ cells around arterioles were negative for SM22 or αSMA (Figures 1E and S1C).

We observed little LepR antibody staining in CD45$^+$ or Ter119$^+$ hematopoietic cells (Figure 1F) or in VE-Cad$^+$ bone marrow endothelial cells (Figures 1A, 1E, and 1G). The rare LepR antibody staining that was observed in these cells may reflect the expression of short isoforms of *Lepr* that lack the intracellular signaling domain (*Ob–Ra*, *Ob–Rc*, *Ob–Rd*, and *Ob–Re*). These isoforms are somewhat more broadly expressed than the *Ob–Rb* isoform, which encodes full-length LepR, including the intracellular signaling domain. It is this full-length isoform whose expression is marked by *Lepr-cre*. Little recombination was observed in macrophages (Figure S1D) or in other hematopoietic cells (Figure 1M) using *Lepr-cre*.

Consistent with the lack of EYFP expression in bone-lining cells from 2-month-old *Lepr-cre; EYFP* reporter mice (Ding et al., 2012), we were unable to detect LepR antibody staining in *Col2.3*-GFP$^+$ osteoblastic cells from cortical or trabecular bone in 2-month-old mice (Figure 1H). Neither Aggrecan$^+$ articular cartilage cells in the femur (knee joint; Figure 1I) nor Perilipin$^+$ fat cells in the bone marrow (Figure 1J) exhibited LepR antibody staining. Thus, at 2 months of age, LepR expression was largely restricted to perivascular stromal cells and not to more differentiated mesenchymal derivatives in bone marrow.

Consistent with the LepR antibody staining and *Lepr-cre; tdTomato* conditional reporter expression pattern, quantitative real-time PCR (qPCR) showed that full-length *Ob-Rb* transcripts were at 100- to 1,000-fold higher levels in PDGFRα$^+$ CD45$^-$Ter119$^-$CD31$^-$ perivascular stromal cells as compared to unfractionated bone marrow cells, *Col2.3*-GFP$^+$CD45$^-$ Ter119$^-$ osteoblastic cells, and VE-Cad$^+$CD45$^-$Ter119$^-$ bone marrow endothelial cells (Figure 1K). Virtually all LepR$^+$ cells expressed *Scf*-GFP and nearly all *Scf*-GFP$^+$ cells expressed LepR (Figure S1E). LepR$^+$ *Scf*-GFP$^-$ cells around certain arterioles appeared to represent <1% of LepR$^+$ cells in bone marrow (Figure 1E). Nearly all LepR$^+$ cells expressed high levels of *Cxcl12*-DsRed and nearly all cells that expressed high levels of *Cxcl12*-DsRed expressed LepR (Figure S1F). Most LepR$^+$ cells expressed low levels of *Nestin*-GFP (Figures S1G and S1H), consistent with a recent report (Kunisaki et al., 2013). Cells that expressed high levels of *Nestin*-GFP did not stain with either LepR or PDGFRα (Figure S1H). The vast majority of bone marrow cells that express high levels of HSC niche factors and the bone marrow MSC marker PDGFRα are thus LepR$^+$.

LepR$^+$CD45$^-$Ter119$^-$ bone marrow stromal cells accounted for 0.2% to 0.3% of enzymatically dissociated bone marrow cells, irrespective of whether these cells were identified by LepR antibody staining (Figure 1L) or Tomato expression in *Lepr-cre; tdTomato* conditional reporter mice (Figure 1M). Nearly all LepR$^+$CD45$^-$Ter119$^-$CD31$^-$ bone marrow stromal cells were positive for PDGFRα and nearly all PDGFRα$^+$CD45$^-$ Ter119$^-$CD31$^-$ bone marrow cells were LepR$^+$ (Figures 1L and 1M). These data suggested that LepR$^+$ bone marrow stromal cells might be highly enriched for MSCs. Consistent with this possibility, we found that LepR$^+$CD45$^-$Ter119$^-$CD31$^-$ bone marrow stromal cells were uniformly positive for the MSC markers CD51 (Pinho et al., 2013) and PDGFRβ (Komada et al., 2012) (Figure 1N). Approximately 68% of LepR$^+$CD45$^-$ Ter119$^-$ cells were positive for the MSC marker CD105 (Chan et al., 2009; Park et al., 2012) (Figure 1N). LepR$^+$CD45$^-$Ter119$^-$ cells were heterogeneous for Sca-1 (Figure 1N), which is

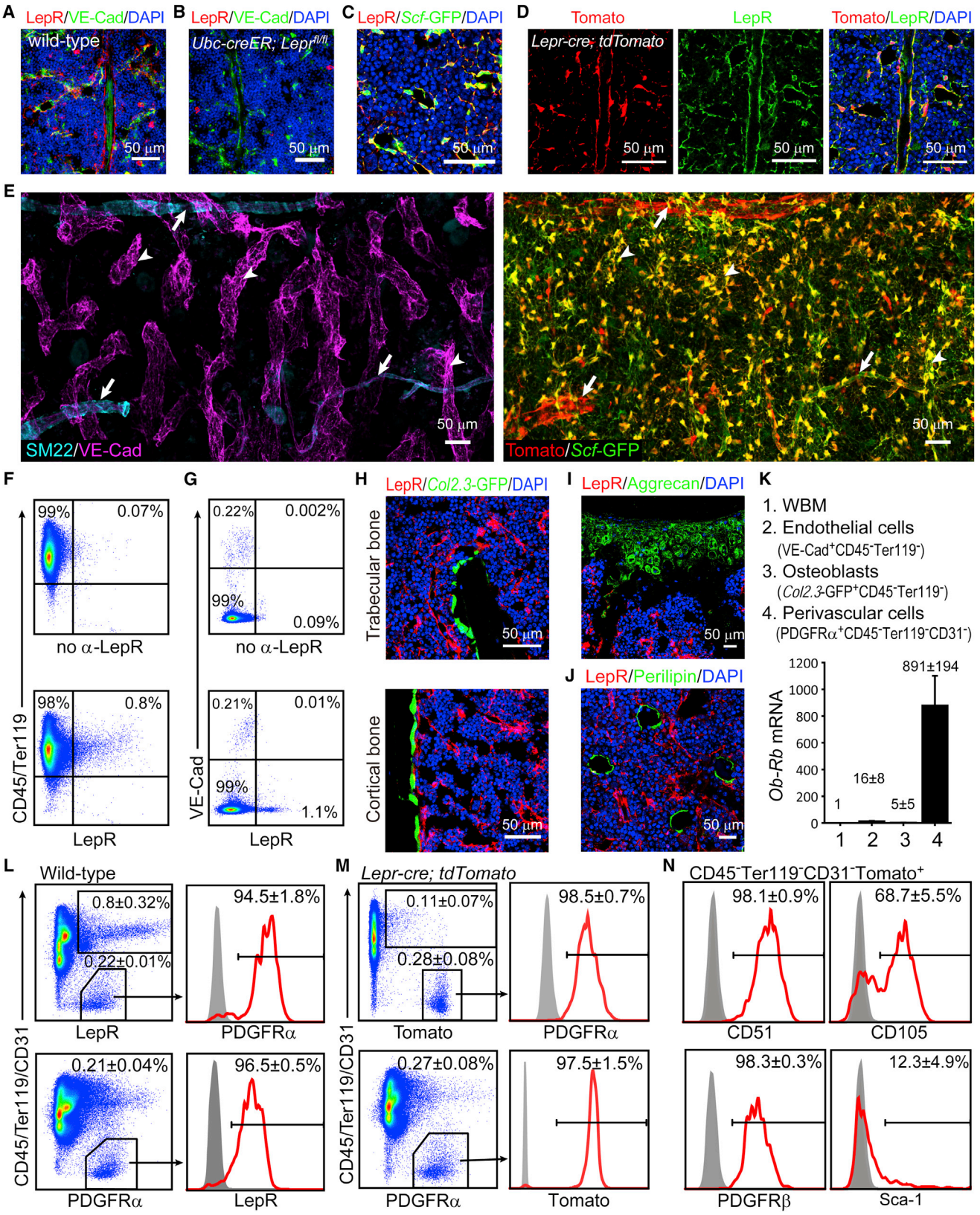

(legend on next page)

expressed by a subset of MSCs (Morikawa et al., 2009; Omatsu et al., 2010).

LepR$^+$ Cells Are the Main Source of CFU-Fs in Bone Marrow

To assess CFU-F activity we enzymatically dissociated bone marrow cells and added them to adherent cultures at clonal density. Figure 2B shows the percentage of cells in each cell population sorted from unfractionated bone marrow cells (including both hematopoietic and stromal elements) that formed CFU-F colonies in culture. Figure 2C shows the percentage of cells in each cell population sorted from nonhematopoietic (CD45$^-$Ter119$^-$) bone marrow stromal cells that formed CFU-F colonies in culture. In our experiments, 0.012% ± 0.002% of all enzymatically dissociated bone marrow cells (Figure 2B) or 1.3% ± 0.5% of CD45$^-$Ter119$^-$ bone marrow stromal cells formed CFU-F colonies (Figure 2C).

Consistent with a prior study (Morikawa et al., 2009), 9.8% ± 5.0% of PDGFRα$^+$CD45$^-$Ter119$^-$ bone marrow stromal cells, 15.6% ± 3.0% of PDGFRα$^+$Sca-1$^+$CD45$^-$Ter119$^-$ bone marrow stromal cells, and 8.3% ± 5.2% of PDGFRα$^+$Sca-1$^-$ CD45$^-$Ter119$^-$ bone marrow stromal cells formed CFU-F colonies (Figure 2C). Although PDGFRα$^+$Sca-1$^+$ stromal cells were more highly enriched for CFU-F activity than PDGFRα$^+$ Sca-1$^-$ cells (Figure 2C), PDGFRα$^+$Sca-1$^-$ stromal cells contained most of the CFU-F activity in the bone marrow (Figure S2A) because they were much more abundant than PDGFRα$^+$Sca-1$^+$ cells (0.22% ± 0.08% versus 0.03% ± 0.02% of bone marrow cells; Figures 1N and S1J). PDGFRα$^+$ bone marrow cells are thus highly enriched for CFU-F, but we could not fate map PDGFRα$^+$ cells because *Pdgfra*-CreER (Rivers et al., 2008) recombined poorly in bone marrow PDGFRα$^+$ cells (data not shown).

The vast majority of bone marrow CFU-Fs derive from LepR$^+$ cells. In CFU-F colonies formed by bone marrow cells from *Lepr-cre; tdTomato* mice, 94% ± 4% were Tomato$^+$ (Figures 2A and S2B–S2E). In 2- to 4-month-old *Lepr-cre; tdTomato* mice, 8.5% ± 2.5% of all Tomato$^+$ bone marrow cells (Figure 2B) and 11% ± 3.5% of Tomato$^+$CD45$^-$Ter119$^-$ bone marrow stromal cells formed CFU-F colonies (Figure 2C), whereas only 0.10% ± 0.08% of Tomato$^-$CD45$^-$Ter119$^-$ bone marrow stromal cells formed CFU-F colonies (Figure 2C). Consistent with a previous study (Park et al., 2012), almost all of the Tomato$^+$ CFU-Fs in *Lepr-cre; tdTomato* bone marrow were CD105$^+$ (Figure 2C). Cells derived from full-length LepR$^+$ cells in the bone marrow were thus as highly enriched for CFU-Fs as PDGFRα$^+$ CD45$^-$Ter119$^-$ bone marrow cells.

We split cells obtained from individual CFU-F colonies formed by LepR$^+$ cells into three aliquots and subcloned them into cultures that promoted bone, cartilage, or fat cell differentiation. In CFU-F colonies formed by Tomato$^+$ bone marrow cells from *Lepr-cre; tdTomato* mice, 8.9 ± 4.5% underwent multilineage differentiation (Figure 2D), giving rise to Alizarin-red-S-stained osteoblastic cells (Figures S2F and S2G), Oil-red-O-stained adipocytes (Figures S2H and S2I), and Toluidine-blue-stained chondrocytic cells (Figures S2J and S2K). Most of the remaining CFU-F colonies formed by Tomato$^+$ cells differentiated to osteoblastic cells with or without chondrocytic cells or fat cells. Overall, 58% ± 17% of all CFU-F colonies formed by Tomato$^+$ cells formed osteoblastic cells in culture.

We also sorted individual LepR$^+$ cells from *Lepr-cre; tdTomato; Col2.3-GFP* mice into culture, allowed them to form CFU-F colonies, then expanded individual colonies, implanted the cells into denatured collagen sponges, transplanted them subcutaneously, and assessed the development of bony ossicles and hematopoiesis 8 weeks later. The presence of hematopoiesis was determined based on the presence of undifferentiated and differentiated erythroid, myeloid, and lymphoid cells in ossicle sections. Fourteen of twenty-five sponges did not form bone. Of the 11 that did form bone, we detected hematopoiesis in 8 (Figures 2D and S2L–S2N), 3 of which had abundant hematopoiesis that resembled bone marrow and 5 of which had smaller foci of hematopoietic cells distributed throughout each ossicle. In each case, we observed donor-derived

Figure 1. LepR and *Scf*-GFP-Expressing Cells Are Abundant around Sinusoids throughout the Bone Marrow and Are Distinct from Other Stromal Cells

(A and B) Representative femur sections from 3- to 4-month-old wild-type (A) and *Ubc-creER; Lepr$^{fl/fl}$* mice (B). The anti-LepR antibody stained perivascular cells in wild-type (A) but not *Ubc-creER; Lepr$^{fl/fl}$* (B) bone marrow (unless otherwise indicated, each panel reflects data from three mice/genotype from three independent experiments).

(C) Staining with anti-LepR antibody and *Scf*-GFP.

(D) Staining with anti-LepR antibody strongly overlapped with Tomato expression around sinusoids and arterioles in the bone marrow of *Lepr-cre; tdTomato* mice.

(E) 3D reconstruction of a Z stack of tiled confocal images of femur bone marrow from a *Lepr-cre; tdTomato; Scf-GFP* mouse. Anti-VE-Cad staining marked sinusoids (arrowheads, left panel) and arterioles while anti-SM22 staining specifically marked arterioles (arrows, left panel). Left and right panels represent images from the same field of view. LepR was expressed by perivascular cells around sinusoids and arterioles, but LepR$^+$*Scf*-GFP$^+$ cells were most abundant around sinusoids. Note that most *Scf*-GFP staining that did not overlap with Tomato staining represented the processes of perivascular cells that had Tomato staining in their cell body (see Figure S1B). The frequency of *Scf*-GFP$^+$ cells appears high in this image because it represents a Z stack of images from a thick section, not a single optical section.

(F and G) Flow cytometry analysis showed that CD45/Ter119$^+$ hematopoietic cells (F) and VE-Cad$^+$ endothelial cells (G) rarely stained positively for LepR. The bone marrow was dissociated mechanically in (F) (thus lacking stroma) or enzymatically in (G) (including stroma).

(H–J) *Col2.3*-GFP$^+$ osteoblasts (H), Aggrecan$^+$ chondrocytes (I), and Perilipin$^+$ adipocytes (J) did not stain with anti-LepR antibody. n = 3–5 mice from at least three independent experiments.

(K) Quantitative RT-PCR of *Ob–Rb* transcript levels (normalized to *β-Actin*). Data represent mean ± SD (standard deviation) from four independent experiments.

(L and M) In 2- to 4-month-old mice, nearly all LepR$^+$ bone marrow cells stained positively for PDGFRα, and vice versa, irrespective of whether the LepR$^+$ cells were identified by antibody staining (L) or Tomato expression in *Lepr-cre; tdTomato* mice (M). The data represent mean ± SD from 3–5 mice from at least three independent experiments.

(N) Marker expression by Tomato$^+$ bone marrow cells from *Lepr-cre; tdTomato* mice.

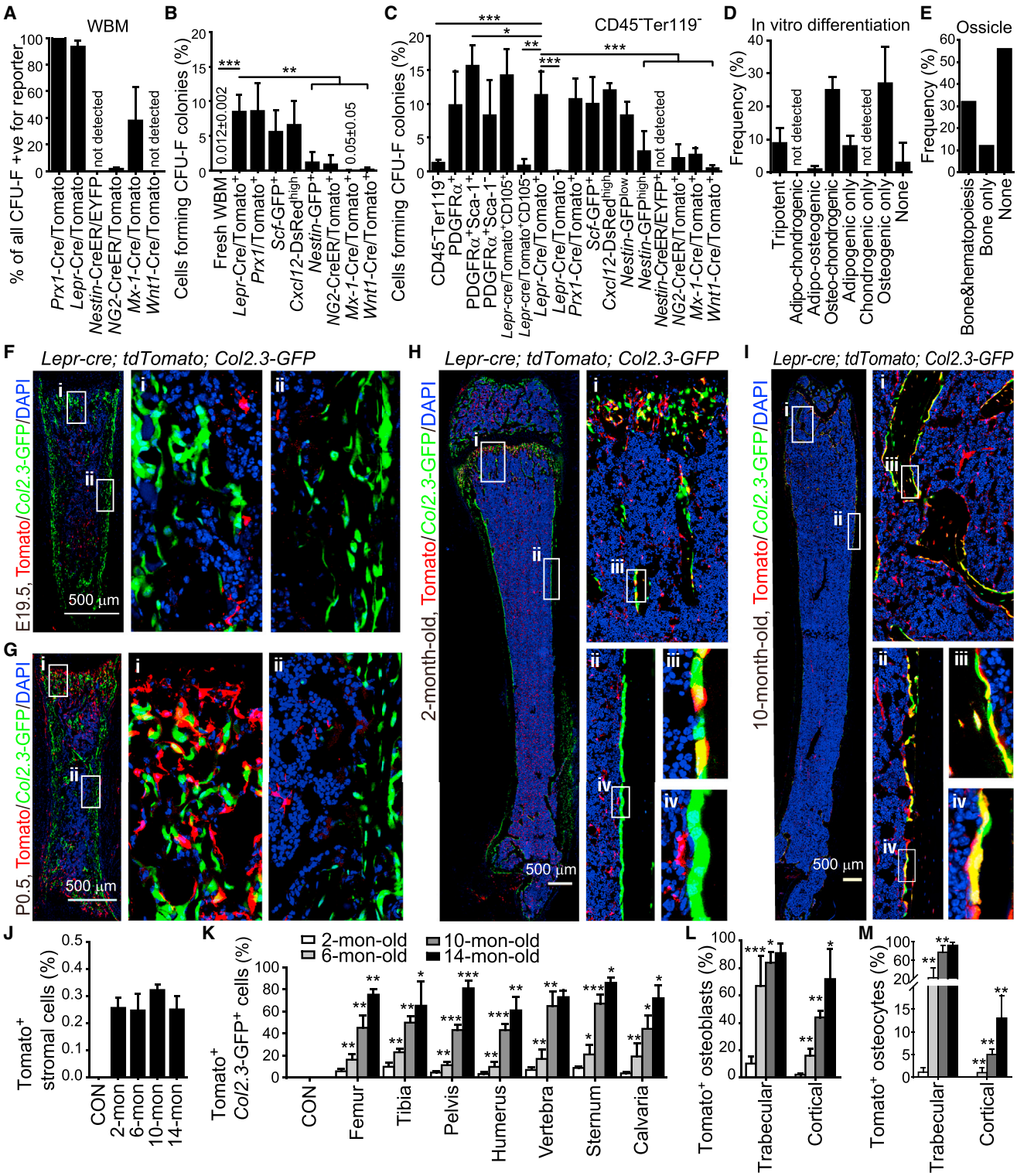

Figure 2. LepR$^+$ Cells Contain Most of the CFU-Fs in Adult Bone Marrow and Are the Major Source of New Bone in Adult Mice

(A) Percentage of all CFU-F colonies that were labeled by conditional reporter expression when cultured from enzymatically dissociated bone marrow of the indicated genotypes. Macrophage colonies were excluded by staining with anti-CD45 antibody in all experiments. n = 3–11 mice/genotype from at least three independent experiments.

(B) Percentage of bone marrow cells expressing each marker that formed CFU-F colonies in culture (n = 3–5 mice/genotype from at least three independent experiments).

(legend continued on next page)

(Tomato$^+$) bone, stromal cells, and adipocytes in addition to host-derived CD45$^+$ hematopoietic cells (Figures S2L and S2M). Cells from the three ossicles that contained the most hematopoietic cells gave multilineage reconstitution of irradiated mice, demonstrating the presence of primitive hematopoietic progenitors (data not shown).

When bone marrow cells were obtained from the femurs and tibias of *Prx1-cre; tdTomato* conditional reporter mice, all CFU-F colonies formed by unfractionated bone marrow cells were Tomato$^+$ (Figure 2A). In 2- to 4-month-old *Prx1-cre; tdTomato* mice, 8.6% ± 4.0% of all Tomato$^+$ bone marrow cells (Figure 2B) and 10% ± 3% of Tomato$^+$CD45$^-$Ter119$^-$ bone marrow stromal cells formed CFU-F colonies (Figure 2C). Nearly all LepR$^+$ antibody stained cells were Tomato$^+$ in *Prx1-cre; tdTomato* mice and nearly all Tomato$^+$ cells were LepR$^+$ (Figures S2P and S2Q). Thus, LepR$^+$ cells in the marrow of limb bones uniformly express the MSC marker *Prx1*.

Consistent with the conclusion that MSCs secrete factors that promote HSC maintenance (Méndez-Ferrer et al., 2010; Omatsu et al., 2010; Sacchetti et al., 2007), both *Scf*-GFP$^+$ bone marrow cells and *Cxcl12*-DsRed^{high} bone marrow cells were highly enriched for CFU-Fs (Figures 2B and 2C). The observation that these cells are similarly enriched for CFU-F and LepR$^+$ cells is consistent with our data demonstrating that nearly all cells that express *Scf*-GFP or high levels of *Cxcl12*-DsRed are LepR$^+$ (Figures S1D and S1E). These data suggest a strong overlap between LepR$^+$ stromal cells and CAR cells in the bone marrow.

CFU-Fs often expressed *Mx1-Cre*, consistent with a recent study (Park et al., 2012). Bone marrow sections from *Mx-1-cre; tdTomato* mice showed widespread Tomato expression among hematopoietic cells, vascular cells, perivascular cells, and bone-lining osteoblastic cells (Figures S4B–S4D). We found that 37% ± 25% of all CFU-F colonies formed by *Mx-1-cre; tdTomato* bone marrow cells were Tomato$^+$ (Figure 2A) and 46% ± 23% of all CD45$^-$Ter119$^-$CD31$^-$PDGFRα^+ stromal cells were Tomato$^+$ (Figure S4A). Only rare Tomato$^+$ bone marrow cells formed CFU-F colonies (Figures 2B and 2C) due to widespread recombination among hematopoietic cells and other stromal cells (Figure S4A).

CFU-Fs rarely expressed *NG2*-CreER. Only 1.8% ± 1.0% of CFU-F colonies formed by bone marrow cells from *NG2-creER; tdTomato* reporter mice were Tomato$^+$ (Figure 2A). Tomato$^+$ cells accounted for 0.0026% ± 0.007% of all bone marrow cells in *NG2-creER; tdTomato* mice and 8.8% ± 3.6% of these cells stained positively for the MSC marker PDGFRα (Figure S3A). Only 9.8% ± 3.4% of Tomato$^+$ bone marrow cells in *NG2-creER; tdTomato; Scf-GFP* mice were positive for *Scf*-GFP (Figure S3A). We observed almost no *NG2*-CreER-expressing cells among PDGFRα^+ cells or *Scf*-GFP$^+$ cells in the bone marrow (Figures S3B–S3D).

In the bone marrow, *NG2-creER* labeled vascular smooth muscle cells (Figure S3E) and GFAP$^+$ glia associated with nerve fibers (Figure S3F), chondrocytes, osteocytes, and rare osteoblasts (data not shown). NG2-antibody-stained cells also included Aggrecan$^+$ chondrocytes (Figure S3G), *Col2.3*-GFP$^+$ osteoblasts, and osteocytes (Figure S3H) in 2-month-old mice. Smooth muscle cells (Murfee et al., 2005), peripheral nerve Schwann cells (Schneider et al., 2001), cartilaginous cells, and osteoblasts (Fukushi et al., 2003) have all been previously reported to express NG2.

CFU-Fs also rarely expressed *Nestin-creER*. We did not detect any EYFP$^+$ CFU-F colonies formed by bone marrow cells from *Nestin-creER; loxp-EYFP* mice (Figure 2A). We observed labeling of rare cells associated with some arterioles in the bone marrow of *Nestin-creER; loxp-EYFP* mice (Figure S4F) consistent with previously published images (Méndez-Ferrer et al., 2010). EYFP$^+$ cells accounted for 0.0012% ± 0.0005% of bone marrow cells and were nearly uniformly negative for PDGFRα (Figure S4E). When we aged *Nestin-creER; loxp-EYFP* mice for 11 months, we only detected rare EYFP$^+$ osteoblasts (Figure S4F), demonstrating that *Nestin*-CreER-expressing cells are not a significant source of bone in vivo.

The observation that *Nestin*-GFP$^+$ cells included CFU-Fs, but that *Nestin*-CreER-expressing cells did not (Figures 2C and S1H), is consistent with our observation that different *Nestin* transgenes exhibit different expression patterns in the bone marrow (Ding et al., 2012). Neither *Nestin*-GFP^{low} nor *Nestin*-GFP^{high} bone marrow cells appear to express endogenous *Nestin* (see microarray data in Méndez-Ferrer et al., 2010 and RNaseq data in Kunisaki et al., 2013).

CFU-Fs were not neural crest-derived based on fate mapping with *Wnt1-Cre* (Chai et al., 2000; Echelard et al., 1994; Joseph et al., 2004). We observed Tomato$^+$ nerve fibers and glia in the bone marrow of *Wnt1-cre; tdTomato* mice (Figure S4H), confirming that neural-crest-derived cells were marked in the bone marrow. In 2- to 4-month-old *Wnt1-cre; tdTomato* mice, 0.17% ± 0.29% of all Tomato$^+$ bone marrow cells (Figure 2B) and 0.5% ± 0.5% of Tomato$^+$CD45$^-$Ter119$^-$ cells (Figure 2C)

(C) Percentage of nonhematopoietic (CD45$^-$Ter119$^-$) bone marrow cells expressing each marker that formed CFU-F colonies in culture (n = 3–11 mice/genotype from at least three independent experiments). Two-tailed Student's t tests were used to assess statistical significance. *p < 0.05, **p < 0.01, ***p < 0.001.

(D) The percentage of CFU-F colonies that arose from Tomato$^+$CD45$^-$Ter119$^-$CD31$^-$ cells from *Lepr-cre; tdTomato* mice that gave rise to Oil red O$^+$ adipocytes, Toluidine blue$^+$ chondrocytes, and/or Alizarin red S$^+$ osteoblasts (n = 3 mice from three independent experiments).

(E) Development of bone and hematopoiesis in ossicles formed by individual CFU-F colonies that arose from LepR$^+$ stromal cells from four *Col2.3-GFP; Lepr-cre; tdTomato* mice.

(F–I) Representative femur sections from *Lepr-cre; tdTomato; Col2.3-GFP* mice of different ages showing the increasing generation of Tomato$^+$*Col2.3*-GFP$^+$ osteoblasts with age (three to five mice/age from at least four independent experiments).

(J) The frequency of Tomato$^+$CD45$^-$Ter119$^-$CD31$^-$*Col2.3*-GFP$^-$ bone marrow stromal cells in the femurs of *Lepr-cre; tdTomato; Col2.3-GFP* mice did not change with age. Cells from ~6-month-old *Col2.3-GFP; tdTomato* mice were negative controls (CON). Data in all remaining panels represent mean ± SD from three to five mice/age from at least three independent experiments.

(K) Percentage of *Col2.3*-GFP$^+$ osteoblasts that were also Tomato$^+$ in enzymatically dissociated bone from *Lepr-cre; tdTomato; Col2.3-GFP* mice of different ages. Osteoblasts from age-matched *Col2.3-GFP* or *Col2.3-GFP; tdTomato* mice were used as negative controls in each experiment (CON). Two-tailed Student's t tests were used to assess statistical significance among consecutive ages. *p < 0.05, **p < 0.01, ***p < 0.001.

(L and M) Percentage of osteoblasts (L) and osteocytes (M) that were Tomato$^+$ in bone sections from *Lepr-cre; tdTomato; Col2.3-GFP* mice.

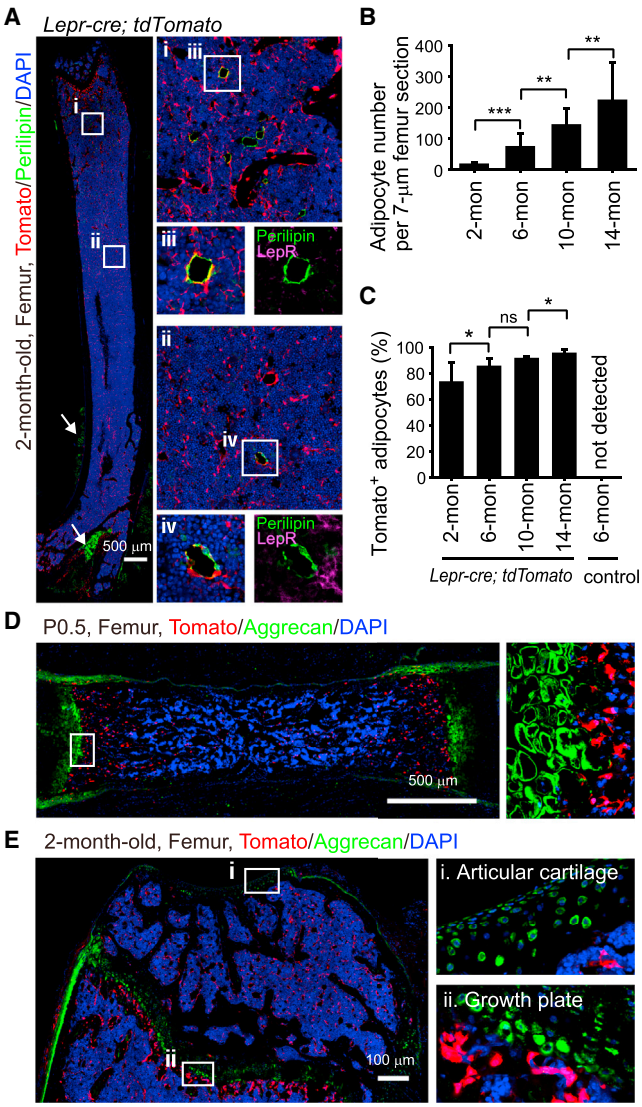

Figure 3. LepR$^+$ Cells Give Rise to Most Bone Marrow Adipocytes but Few Chondrocytes

(A) Representative femur sections from a 2-month-old *Lepr-cre; tdTomato* mouse. Perilipin$^+$ adipocytes in the bone marrow did not stain with an anti-LepR antibody (purple) but were Tomato$^+$ (red). Periosteal adipocytes (arrows) were uniformly Tomato$^-$ (representative of four mice from four independent experiments).

(B and C) Quantification of adipocyte number per 7 μm femur section (B) and the percentage of adipocytes that were Tomato$^+$ at each age (C) in *Lepr-cre; tdTomato* mice. Two-tailed Student's t tests were used to assess statistical significance. ns, not significant; *$p < 0.05$, **$p < 0.01$, ***$p < 0.001$. n = 3–5 mice/age from at least three independent experiments. Data represent mean ± SD.

(D and E) Aggrecan$^+$ chondrocytes were not Tomato$^+$ in P0.5 (D) or 2-month-old (E) *Lepr-cre; tdTomato* mice (n = 3–5 mice/age from at least three independent experiments).

formed CFU-F colonies. However, none of the CFU-F colonies formed by unfractionated bone marrow cells from *Wnt1-cre; tdTomato* reporter mice were Tomato$^+$ (Figure 2A). Tomato$^+$ cells in the bone marrow of 2-month-old *Wnt1-cre; tdTomato* reporter mice accounted for only 0.0017% ± 0.001% of bone marrow cells and were mostly negative for the MSC marker PDGFRα (Figure S4G). We aged *Wnt1-cre; tdTomato* mice for 5 months and observed rare Tomato$^+$ osteocytes (Figure S4H) but no Tomato$^+$ osteoblasts, indicating that these cells are not a significant source of bone-forming progenitors in young adult mice.

LepR$^+$ Cells Are a Major Source of Bone in Adult Mice

LepR$^+$ cells arose perinatally in bone marrow and made little bone before 2 months of age. We fate mapped the LepR$^+$ cells in vivo using *Lepr-cre; tdTomato; Col2.3-GFP* mice in which osteoblastic bone-lining cells can be unambiguously identified based on *Col2.3-GFP* expression (Kalajzic et al., 2002). At embryonic day (E) 19.5, Tomato$^+$ cells were rare in the bone marrow of *Lepr-cre; tdTomato; Col2.3-GFP* mice and we observed no contribution of these cells to bone (Figure 2F). By postnatal day (P) 0.5, there was a sharp increase in the number of Tomato$^+$ cells in metaphyseal bone marrow, though Tomato$^+$ cells remained rare in the diaphyseal bone marrow and only rare Tomato$^+$*Col2.3*-GFP$^+$ osteoblasts were observed in trabecular bone (Figure 2G). By 2 months of age, Tomato$^+$ cells were visible throughout the bone marrow in both metaphysis and diaphysis, but Tomato$^+$*Col2.3*-GFP$^+$ cells remained infrequent (Figure 2H), accounting for 3%–10% of *Col2.3*-GFP$^+$ cells in several bones (Figure 2K). However, the contribution of LepR$^+$ cells to bone increased sharply with age. Tomato$^+$ cells accounted for 10%–23% of *Col2.3*-GFP$^+$ cells in several bones at 6 months of age, 43%–67% of *Col2.3*-GFP$^+$ cells at 10 months of age, and 61%–81% of *Col2.3*-GFP$^+$ cells at 14 months of age (Figures 2K and S2R). The increased frequency of Tomato$^+$*Col2.3*-GFP$^+$ cells was not caused by the induction of *Lepr* expression within *Col2.3*-GFP$^+$ osteoblastic cells (Figures S2S and S2T).

By 10 months of age, Tomato$^+$ cells contributed not only to bone-lining osteoblastic cells but also to osteocytes within the bone matrix (Figure 2Iiii). The percentage of osteocytes that were Tomato$^+$ increased significantly with age, but much more rapidly within trabecular bone (Figure 2M). Tomato$^+$ cells represented 92% ± 7% of osteocytes in trabecular bone and 13% ± 5% of osteocytes in cortical bone at 14 months of age.

LepR$^+$ Cells Are a Major Source of Adipocytes in Adult Bone Marrow

Although LepR antibody did not detectably stain Perilipin$^+$ adipocytes (Figures 1J and 3A), most Perilipin$^+$ adipocytes in the bone marrow of 2- to 14-month-old *Lepr-cre; tdTomato* mice were Tomato$^+$ (Figures 3A–3C). The number of adipocytes in the bone marrow increased dramatically with age (Figure 3B). In contrast to those in the bone marrow, periosteal adipocytes (outside of the marrow cavity) were all negative for Tomato (Figure 3A), suggesting a distinct cellular origin. LepR$^+$ cells are thus the major source of adipocytes in adult bone marrow.

Chondrogenesis is active during fetal development but largely inactive throughout adulthood (Raghunath et al., 2005). In mice at P0.5 and at 2 months of age, we detected no Tomato expression among Aggrecan$^+$ chondrocytes in the femurs of *Lepr-cre; tdTomato* mice (Figure 3D) in spite of Tomato$^+$ osteoblasts and perivascular stromal cells adjacent to the growth plate (Figure 3E). In 6-, 10-, and 14-month-old mice, we remained unable to detect Tomato$^+$ chondrocytes in articular cartilage or growth plate cartilage associated with femurs and tibias (Figure S5A

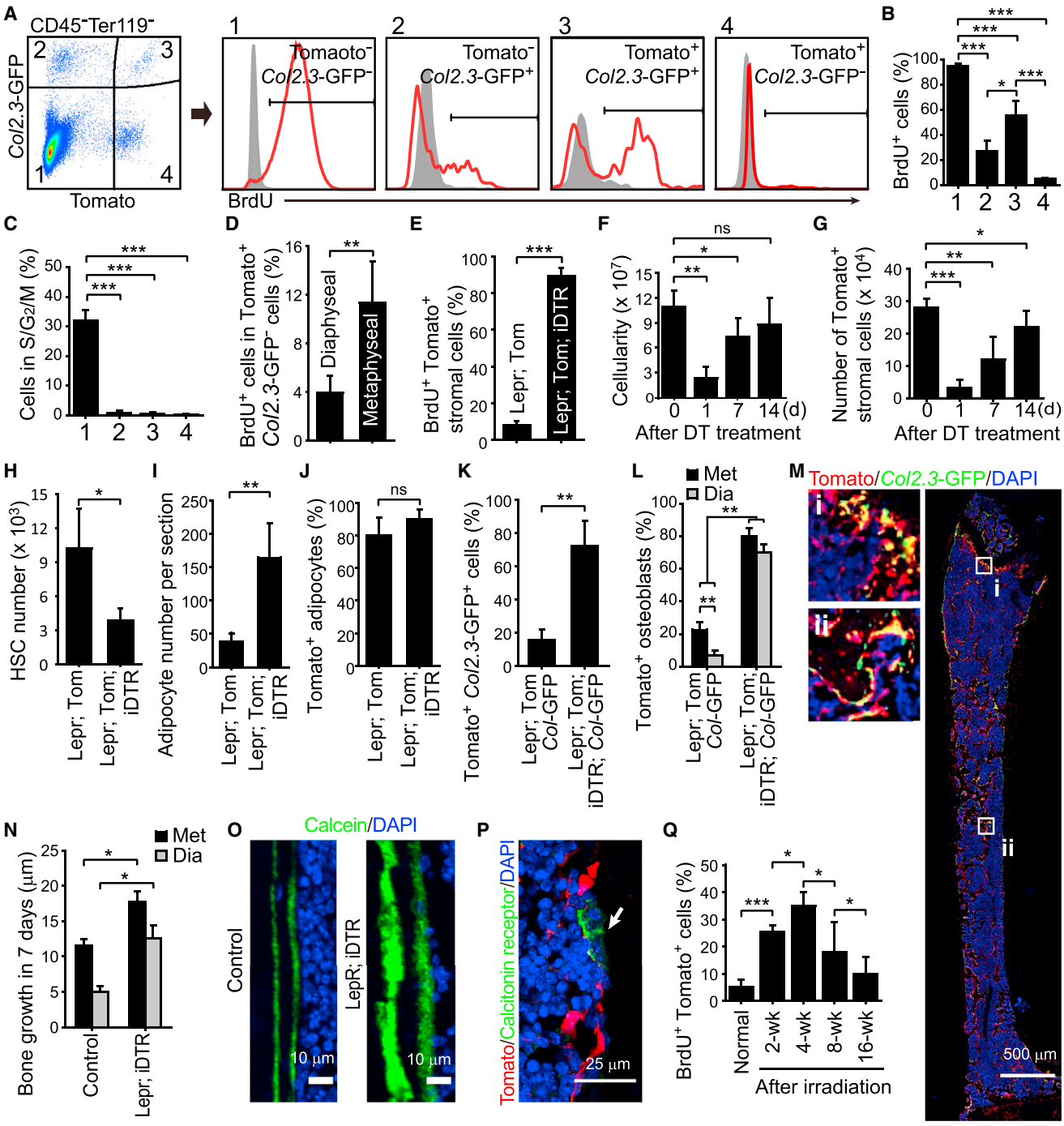

Figure 4. LepR$^+$*Col2.3*-GFP$^-$ Cells Are Quiescent under Normal Physiological Conditions in Adult Bone Marrow but Go into Cycle to Regenerate Bone after Injury

(A–C) BrdU incorporation (14 day pulse) (A and B) or Hoechst staining (C) by various stromal cell fractions from enzymatically dissociated bone and bone marrow obtained from 2-month-old *Lepr-cre; tdTomato; Col2.3-GFP* mice. Unless otherwise indicated, data in all remaining panels represent mean ± SD from three or four mice in three independent experiments, with statistical significance assessed by two-tailed Student's t tests. ns, not significant; *$p < 0.05$, **$p < 0.01$, ***$p < 0.001$.

(D) Percentage of Tomato$^+$*Col2.3*-GFP$^-$CD45$^-$Ter119$^-$CD31$^-$ bone marrow stromal cells that incorporated a 14 day pulse of BrdU.

(E) Percentage of Tomato$^+$CD45$^-$Ter119$^-$CD31$^-$ bone marrow stromal cells that incorporated a 14 day pulse of BrdU in femurs and tibias from *Lepr-cre; tdTomato* mice and *Lepr-cre; tdTomato; iDTR* mice 2 weeks after diphtheria toxin (DT) treatment.

(F) Bone marrow cellularity in the femurs and tibias of *Lepr-cre; tdTomato; iDTR* mice at the indicated time points after DT treatment.

(G) Number of Tomato$^+$CD45$^-$Ter119$^-$CD31$^-$ stromal cells in bone marrow from *Lepr-cre; tdTomato; iDTR* mice after DT treatment.

(H) Number of CD150$^+$CD48$^-$Lineage$^-$Sca-1$^+$c-kit$^+$ HSCs in the femurs and tibias 7 days after DT treatment.

(legend continued on next page)

and data not shown). We did observe an increasing contribution with age of Tomato$^+$ cells to a layer of Aggrecan$^-$ cells on the cartilage surface that appeared to be part of the synovial membrane (Figures S5Ai and S5B). We do not know whether Tomato$^+$ synovial cells are lineally related to LepR$^+$ bone marrow stromal cells. Overall, we observed little contribution of LepR$^+$ cells to cartilage.

LepR$^+$ Bone Marrow Stromal Cells Are Quiescent

We administered bromo-deoxyuridine (BrdU) to 2-month-old *Lepr-cre; tdTomato; Col2.3-GFP* mice for 14 days. We found that 94% ± 2.4% of Tomato$^-$*Col2.3*-GFP$^-$ stromal cells were BrdU$^+$, 27% ± 8.9% of Tomato$^-$*Col2.3*-GFP$^+$ osteoblasts were BrdU$^+$, and 55% ± 12% of Tomato$^+$*Col2.3*-GFP$^+$ osteoblasts were BrdU$^+$, but only 4.8% ± 1.1% of Tomato$^+$*Col2.3*-GFP$^-$ stromal cells were BrdU$^+$ (Figures 4A and 4B). Consistent with this, only 0.23% ± 0.3% of Tomato$^+$*Col2.3*-GFP$^-$ stromal cells had greater than 2N DNA content by Hoechst staining (Figure 4C). LepR$^+$ stromal cells are thus largely quiescent in normal adult bone marrow.

At 2 months of age, the LepR$^+$ cells gave rise to osteoblasts and adipocytes to a much greater extent in metaphyseal bone marrow than in diaphyseal bone marrow (Figures 2H, 2L, and 3A). Tomato$^+$*Col2.3*-GFP$^-$ cells from the metaphysis incorporated a 14-day pulse of BrdU at nearly three times the rate of Tomato$^+$*Col2.3*-GFP$^-$ cells from the diaphysis (Figure 4D). Thus, there is regional regulation of LepR$^+$ stromal cells in the bone marrow.

We ablated LepR$^+$ bone marrow cells by administering DT to *Lepr-cre; tdTomato; Rosa26-loxP-stop-loxP-iDTR* (inducible DT receptor) mice and littermate controls. In contrast to DT-treated controls (lacking *iDTR*), in which only 8.2% ± 2.0% of Tomato$^+$*Col2.3*-GFP$^-$ bone marrow stromal cells incorporated a 14-day pulse of BrdU, 89% ± 4.5% of Tomato$^+$ CD45$^-$Ter119$^-$CD31$^-$ cells from *Lepr-cre; tdTomato; iDTR* mice incorporated BrdU (Figure 4E). Bone marrow cellularity and the number of Tomato$^+$ stromal cells in the bone marrow declined significantly 1 day after DT treatment but rebounded within 2 weeks (Figures 4F and 4G). Consistent with our demonstration that LepR$^+$ stromal cells are critical for the maintenance of quiescent HSCs (Ding and Morrison, 2013; Ding et al., 2012; Oguro et al., 2013), DT treatment depleted CD150$^+$CD48$^-$LSK HSCs (Figure 4H).

Within 14 days of DT treatment, adipogenesis (Figure 4J) and osteogenesis (Figure 4K) increased profoundly in the bone marrow. Trabecular bone began filling up the marrow cavity, including the diaphysis (Figure 4M). Virtually all of the bone marrow adipocytes as well as the new *Col2.3*-GFP$^+$ osteoblasts were Tomato$^+$ (Figures 4J–4L). The rate of bone formation, as measured by calcein labeling, was significantly higher in *Lepr-cre; tdTomato; iDTR* mice as compared to controls in both the metaphysis and the diaphysis (Figures 4N and 4O). LepR$^+$ cells did not give rise to Calcitonin$^+$ osteoclasts (Figure 4P). The regeneration of LepR$^+$ cells after ablation is thus associated with increased adipogenesis and osteogenesis.

LepR$^+$ Cells Are Activated by Irradiation to Form Osteoblasts and Adipocytes

We found that 25% ± 2.3% of the Tomato$^+$ stromal cells incorporated BrdU over a 2 week period after irradiation of *Lepr-cre; tdTomato* mice (Figure 4Q). In the next 2 weeks after irradiation, the percentage of Tomato$^+$ stromal cells that incorporated BrdU significantly increased to 35% ± 5.0% (Figure 4Q). At subsequent time points the percentage of Tomato$^+$ stromal cells that incorporated BrdU significantly declined (Figure 4Q). LepR$^+$ cells therefore divide transiently after irradiation. We observed a substantial increase in adipocyte frequency within the bone marrow after irradiation (Figure 5A) and 95% ± 3.0% of the Perilipin$^+$ adipocytes were Tomato$^+$ (Figure 5B). The frequency of osteoblasts undergoing cell death significantly increased 2 days after irradiation (Figure 5C). By 16 weeks after irradiation, most (65% ± 11%) osteoblasts derived from LepR$^+$ cells (Figure 5D and Figure S6A). Irradiation did not activate LepR expression in osteoblasts (Figures S6B and S6C). We remained unable to detect any contribution of LepR$^+$ cells to chondrocytes after irradiation (Figure S6D and data not shown).

Regeneration of Fractured Bone by LepR$^+$ Cells

Two weeks after a break was created in the tibia of two-month-old *Lepr-cre; tdTomato; Col2.3-GFP* mice (Figure 5E), a substantial increase of Tomato$^+$ stromal cells was observed in the marrow cavity adjacent to the fracture site (Figure 5F). *Col2.3*-GFP$^+$ cells close to periosteum were mostly negative for Tomato expression, but much of the callus was composed of Tomato$^+$ cells (Figure 5F). Tomato$^+$ cells accounted for 46% ± 13% of Aggrecan$^+$ chondrocytes in the soft callus 2 weeks following the fracture (Figures 5I and 5J). At 2 and 8 weeks after the fracture, 45% ± 5% and 85% ± 10% of *Col2.3*-GFP$^+$ osteoblasts were Tomato$^+$ (Figures 5F–5H). In contrast, only 9%–14% of *Col2.3*-GFP$^+$ osteoblasts were Tomato$^+$ in the undamaged tibia of the same mice (Figure 5H). We confirmed by qRT-PCR that *Ob–Rb* mRNA was not expressed by newly generated osteoblasts at the tibia fracture site (Figure S6E). Most of the osteoblasts and osteocytes that persisted long-term at the fracture site thus arose from LepR$^+$ cells.

To investigate the contribution of LepR$^+$ cells to the repair of perforated cartilage, we performed a subchondral perforation in articular cartilage associated with the femur in the knee of

(I and J) Quantification of adipocyte number per 7 μm femur section (I) and the percentage of adipocytes that were Tomato$^+$ (J) 14 days after DT treatment.
(K) Percentage of *Col2.3*-GFP$^+$ osteoblasts that were also Tomato$^+$ in enzymatically dissociated bone 2 weeks after DT treatment.
(L) Percentage of *Col2.3*-GFP$^+$ osteoblasts that were also Tomato$^+$ at metaphyseal (Met) and diaphyseal (Dia) bones 2 weeks after diphtheria toxin treatment.
(M) Representative femur sections from *Lepr-cre; tdTomato; Col2.3-GFP; iDTR* mice at 2 weeks after DT treatment. Note the formation of ectopic trabecular bone by Tomato$^+$*Col2.3*-GFP$^+$ cells in the diaphyseal bone marrow cavity (Mii).
(N and O) Bone formation rate in *Lepr-cre; iDTR* and control mice after DT treatment. Two doses of calcein were injected at day 0 and 7 after DT treatment and the distance between calcein bands was measured at 14 days after DT treatment.
(P) Osteoclasts (arrow) were not labeled by Tomato in *Lepr-cre; tdTomato* mice.
(Q) Percentage of Tomato$^+$CD45$^-$Ter119$^-$CD31$^-$ bone marrow stromal cells that incorporated a 14 day pulse of BrdU in *Lepr-cre; tdTomato* mice at various times after irradiation. n = 3–5 mice/time point from three independent experiments.

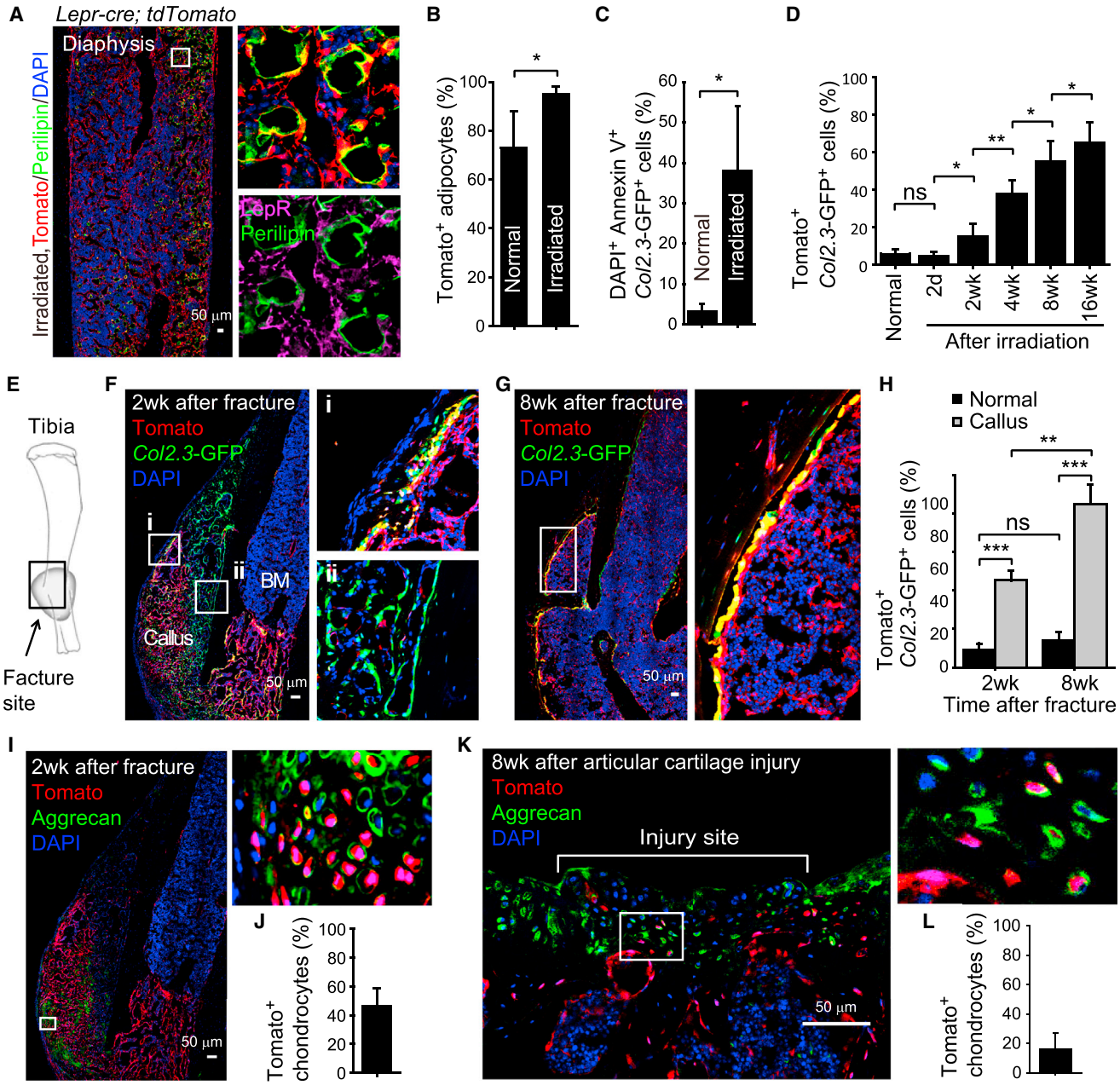

Figure 5. LepR$^+$ Cells Are the Major Source of New Osteoblasts and Adipocytes during Tissue Regeneration and Can also Form Chondrocytes after Subchondral Perforation

(A and B) Representative femur section from a 2-month-old *Lepr-cre; tdTomato* mouse 14 days after lethal irradiation and transplantation of wild-type bone marrow cells. Perilipin$^+$ adipocytes in the bone marrow did not stain with an anti-LepR antibody (purple) but were Tomato$^+$ (red), demonstrating that they derived from endogenous radio-resistant LepR$^+$ cells (mean ± SD from five mice in four independent experiments).

(C) Percentage of *Col2.3*-GFP$^+$ osteoblasts that were also DAPI$^+$Annexin V$^+$ in enzymatically dissociated bone 2 days after irradiation. Data in all remaining panels represent mean ± SD from three or four mice (per time point) in three independent experiments.

(D) Percentage of *Col2.3*-GFP$^+$ osteoblasts that were also Tomato$^+$ in enzymatically dissociated bone from *Lepr-cre; tdTomato; Col2.3-GFP* mice at various time points after irradiation.

(E) Schematic of experimental fracture site. The black rectangle depicts the region shown in images in (G), (H), and (J).

(F and G) Tomato expression by *Col2.3*-GFP$^+$ osteoblasts at the fracture site in *Lepr-cre; tdTomato; Col2.3-GFP* mice at 2 weeks (F) or 8 weeks (G) after fracture.

(H) Percentage of *Col2.3*-GFP$^+$ osteoblasts that were also Tomato$^+$ in unfractured tibias from control mice (normal) and bone callus from *Lepr-cre; tdTomato; Col2.3-GFP* mice.

(I and J) Percentage of Aggrecan$^+$ chondrocytes that were also Tomato$^+$ at the fracture site 2 weeks after the fracture.

(K and L) Percentage of Aggrecan$^+$ chondrocytes that were also Tomato$^+$ 8 weeks after subchondral perforation of articular cartilage in *Lepr-cre; tdTomato* mice.

Statistical significance was always assessed using two-tailed Student's t tests. ns, not significant; *p < 0.05, **p < 0.01, ***p < 0.001.

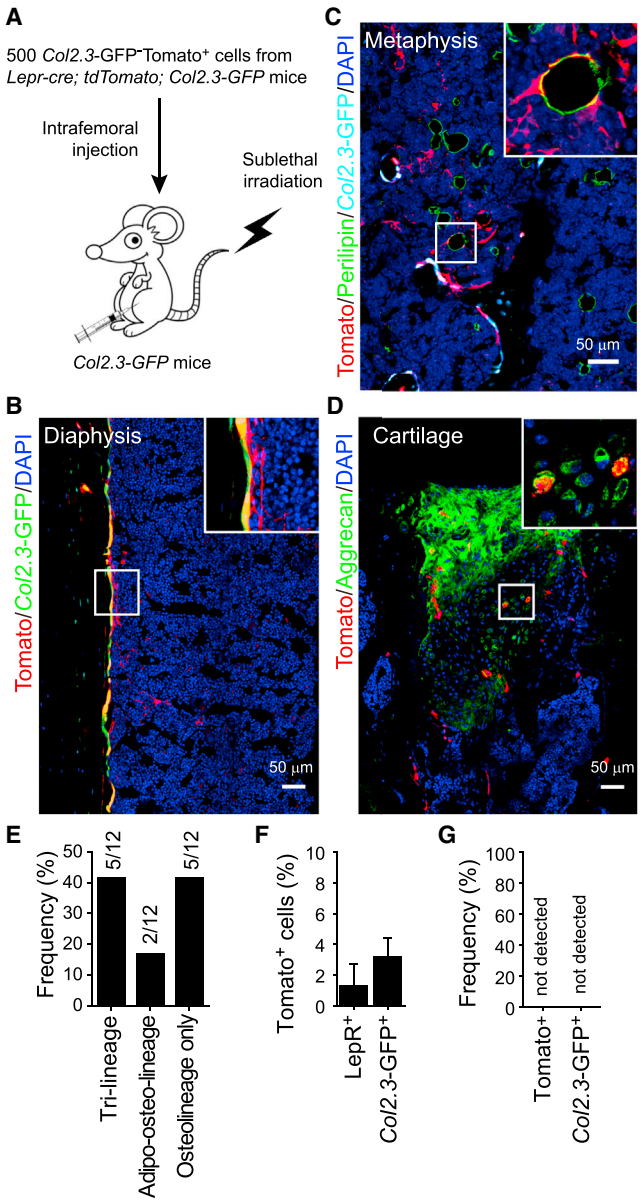

Figure 6. LepR$^+$ Cells Give Rise to Osteoblasts, Adipocytes, and Chondrocytes after Intrafemoral Transplantation

(A) Experimental design.

(B–D) Representative femur sections from *Col2.3-GFP* mice transplanted with 500 Tomato$^+$*Col2.3*-GFP$^-$ cells as described in (A) (n = 5). Note that the transplanted Tomato$^+$*Col2.3*-GFP$^-$ cells gave rise to *Col2.3*-GFP$^+$ osteoblasts (B), Perilipin$^+$ adipocytes (C), and Aggrecan$^+$ cartilage cells (at the injection site, D).

(E) Fraction of recipient mice in which Tomato$^+$ cells were observed to contribute to each of the indicated mesenchymal lineages (n = 12 mice).

(F) The percentage of LepR$^+$ bone marrow stromal cells or *Col2.3*-GFP$^+$ osteoblasts that were also Tomato$^+$ (donor-derived) in the femurs of recipient mice (mean ± SD from three mice in three independent experiments).

(G) No Tomato$^+$LepR$^+$ cells or Tomato$^+$*Col2.3*-GFP$^+$ cells were observed in the femurs of mice transplanted with 10^5 nonhematopoietic *Col2.3*-GFP$^-$Tomato$^-$ cells from *Lepr-cre; tdTomato; Col2.3-GFP* mice (n = 3).

Lepr-cre; tdTomato mice. Eight weeks following perforation, the injured region of the cartilage was covered by Aggrecan$^+$ fibrocartilaginous tissues (Figure 5K) and 16% ± 11% of the Aggrecan$^+$ cells were positive for Tomato expression (Figures 5K and 5L). Thus, LepR$^+$ cells form cartilage after injury even though they contribute little to the formation of cartilage during development.

LepR$^+$ Cells Form Bone, Cartilage, and Adipocytes after Transplantation

We transplanted 500 Tomato$^+$*Col2.3*-GFP$^-$ cells from *Lepr-cre; tdTomato; Col2.3-GFP* mice into sublethally irradiated *Col2.3-GFP* mice by intrafemoral injection (Figure 6A). Four weeks later, Tomato expression was observed in *Col2.3*-GFP$^+$ osteoblasts (Figure 6B), Perilipin$^+$ adipocytes (Figure 6C), and Aggrecan$^+$ chondrocytes in articular cartilage (which had been perforated by the injection; Figure 6D). Of 12 recipient femurs, 5 contained trilineage reconstitution by transplanted Tomato$^+$ cells, 2 contained Tomato$^+$ osteolineage cells and adipocytes, but not cartilage, and 5 contained only Tomato$^+$ osteolineage cells (Figure 6E). In an independent experiment in which engraftment was analyzed by flow cytometry, Tomato$^+$ cells accounted for 1.3% ± 1.4% of LepR$^+$ cells and 3.2% ± 1.2% of *Col2.3*-GFP$^+$ cells in recipient femurs (Figure 6F). In contrast, transplantation of 10^5 Tomato$^-$*Col2.3*-GFP$^-$CD45$^-$Ter119$^-$ stromal cells did not generate any Tomato$^+$ or *Col2.3*-GFP$^+$ cells (Figure 6G), suggesting that LepR$^-$ bone marrow cells have little capacity to form mesenchymal derivatives.

PTEN Regulates Quiescence, Maintenance, and Differentiation of LepR$^+$ Cells

Pten is cell-autonomously required for the maintenance of HSCs (Kalaitzidis et al., 2012; Lee et al., 2010; Magee et al., 2012; Yilmaz et al., 2006; Zhang et al., 2006) and neural stem cells (Bonaguidi et al., 2011). To assess the consequences of *Pten* deletion from MSCs, we generated *Lepr-cre*; *Pten$^{fl/fl}$* mice. As expected, AKT (S473) phosphorylation increased in LepR$^+$ stromal cells isolated from *Lepr-cre*; *Pten$^{fl/fl}$* mice (Figure 7A). Body mass and bone marrow cellularity were normal in *Lepr-cre*; *Pten$^{fl/fl}$* mice (Figures 7B and 7C). However, we observed a more than 2-fold reduction in the frequencies of LepR$^+$ CD45$^-$Ter119$^-$CD31$^-$ stromal cells (Figure 7D), PDGFRα^+ CD45$^-$Ter119$^-$CD31$^-$ stromal cells (Figure 7E), and CFU-Fs (Figure 7F) in *Lepr-cre*; *Pten$^{fl/fl}$* mice relative to littermate controls. Based on BrdU incorporation, LepR$^+$ cells divided more frequently in *Lepr-cre*; *Pten$^{fl/fl}$* mice relative to littermate controls (Figure 7G). *Pten* is thus cell-autonomously required to negatively regulate AKT activation and to maintain normal numbers of quiescent LepR$^+$ MSCs in adult bone marrow.

Four-month-old *Lepr-cre*; *Pten$^{fl/fl}$* mice had a decreased volume of trabecular and cortical bone (Figures 7H–7P) but increased adipogenesis in the metaphysis relative to littermate controls (Figure 7Q). The expression of *Runx2*, a transcription factor required for osteogenesis (Komori et al., 1997; Otto et al., 1997), was markedly reduced in LepR$^+$ stromal cells from *Lepr-cre*; *Pten$^{fl/fl}$* as compared to control mice (Figure 7R). *Pten* deletion did not affect the percentage of CFU-F colonies that contained adipocytes versus osteoblastic cells (Figure 7S), but it did significantly increase the number of

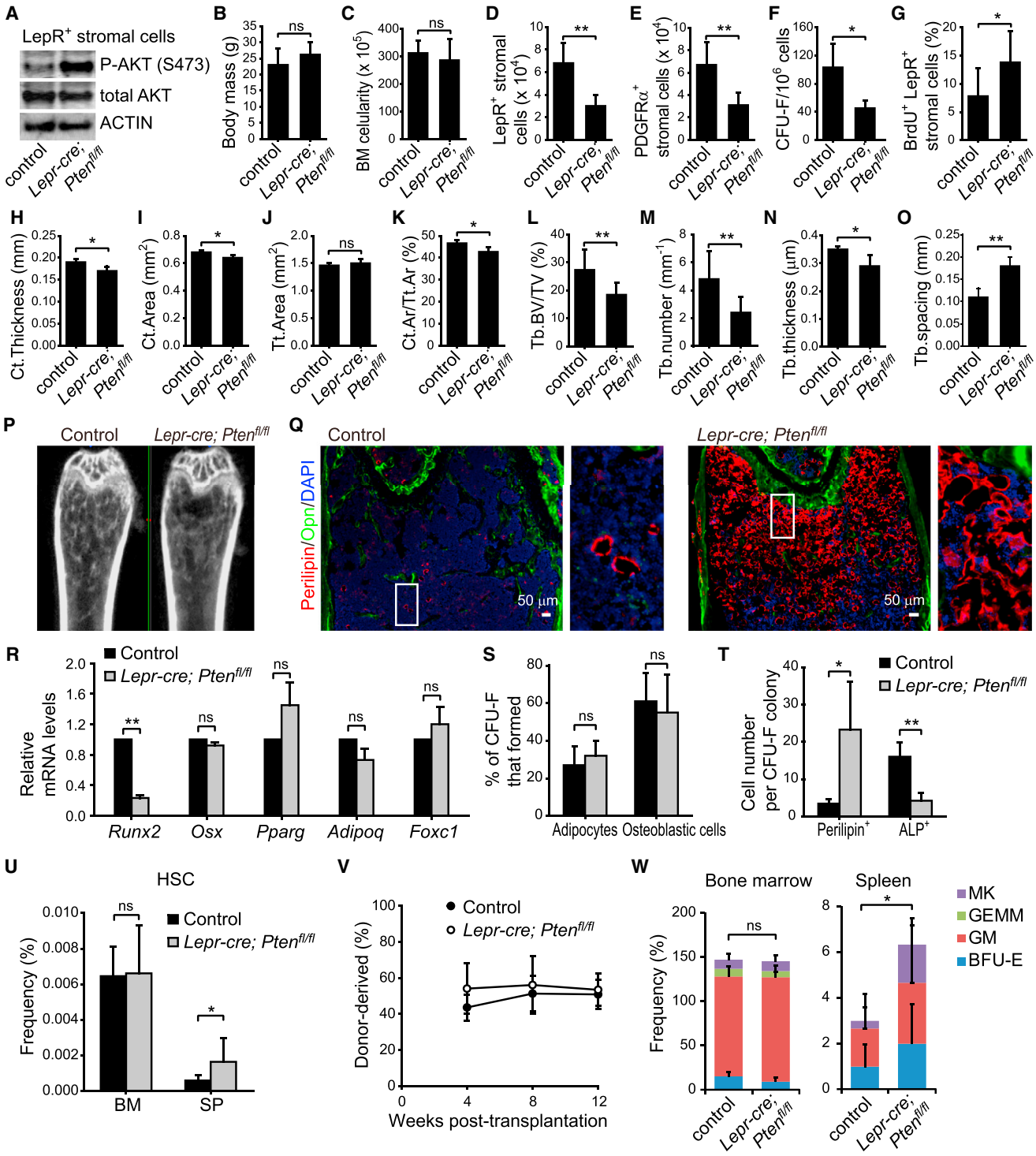

Figure 7. PTEN Regulates Quiescence, Maintenance, and Differentiation in LepR$^+$ Stromal Cells

(A) Representative western blots of flow cytometrically isolated LepR$^+$CD45$^-$Ter119$^-$CD31$^-$ stromal cells from 4-month-old *Lepr-cre; Pten$^{fl/fl}$* mice and littermate controls.

(B) Body mass. (Unless otherwise indicated, all remaining panels show mean ± SD from three to five mice in three to four independent experiments, with statistical significance assessed by two-tailed Student's t tests; ns, not significant; *p < 0.05, **p < 0.01, ***p < 0.001.)

(C) Bone marrow cellularity in the femurs of 4-month-old *Lepr-cre; Pten$^{fl/fl}$* mice and littermate controls.

(D) Number of LepR$^+$CD45$^-$Ter119$^-$CD31$^-$ cells.

(E) Number of PDGFRα$^+$CD45$^-$Ter119$^-$CD31$^-$ cells.

(legend continued on next page)

Perilipin$^+$ adipocytes and significantly reduce the number of alkaline phosphatase$^+$ osteogenic cells that spontaneously differentiated within these colonies (Figure 7T). *Pten* is thus required by LepR$^+$ cells to promote osteogenesis and to restrain adipogenesis.

We did not detect a decline in the frequency of HSCs (Figure 7U) or colony-forming hematopoietic progenitors (Figure 7W and Figures S7B–S7F) in the bone marrow of *Lepr-cre*; *Pten*$^{fl/fl}$ mice. Bone marrow cells from *Lepr-cre*; *Pten*$^{fl/fl}$ and control mice gave similar levels of donor cell reconstitution upon transplantation into irradiated mice (Figures 7V and S7A). Nonetheless, we did observe significant increases in the frequencies of HSCs (Figure 7U) and colony-forming hematopoietic progenitors (Figure 7W) in the spleen. These data suggest that *Pten* deletion from LepR$^+$ bone marrow stromal cells changed the bone marrow niche in a way that led to the mobilization of HSCs and colony-forming progenitors.

DISCUSSION

Our data support the conclusion that MSCs are an important component of the HSC niche (Kunisaki et al., 2013; Méndez-Ferrer et al., 2010; Omatsu et al., 2010; Sacchetti et al., 2007) because LepR$^+$ stromal cells are a major source of HSC niche factors in addition to MSC activity. Nearly all *Scf*-GFP$^+$ bone marrow stromal cells and *Cxcl12*-DsRed^{high} bone marrow stromal cells were LepR$^+$ (Figures 1C, 1E, S1E, and S1F). The high expression of *Cxcl12* (Figure S1E) and PDGFRα (Figures 1L and 1M) by LepR$^+$ stromal cells indicates that these cells overlap strongly with CAR cells, which are also found primarily around sinusoids throughout the bone marrow (Omatsu et al., 2010; Sugiyama et al., 2006). However, our data indicate that *NG2*-CreER-expressing cells are not a significant source of MSCs in the bone marrow. *NG2*-CreER-expressing cells were much more rare than *Scf*-GFP$^+$ cells or *Cxcl12*-DsRed$^+$ cells (Figures S1E, S1F, and S3A–S3C) and we observed little PDGFRα or *Scf*-GFP expression by these cells (Figures S3A–S3D). While Kunisaki et al. (2013) concluded that NG2$^+$Nestin^{high}LepR$^-$ periarteriolar cells express high levels of *Scf* and *Cxcl12*, their RNaseq analysis showed that the "Nestin^{high}LepR$^-$" cells they analyzed were negative for *Nestin* and positive for *Lepr* expression (see GSE48764 in the Gene Expression Omnibus, referenced by Kunisaki et al., 2013). Thus, the data from Kunisaki et al. are consistent with our data indicating that cells with high levels of *Scf* and *Cxcl12* in the bone marrow are marked by LepR.

EXPERIMENTAL PROCEDURES

Mice

All mice were maintained in a C57BL/6 background, including *Lepr-cre* (DeFalco et al., 2001), *Lepr*$^{fl/fl}$ (Cohen et al., 2001), *Pten*$^{fl/fl}$ (Groszer et al., 2001), *Scf-GFP* (Ding et al., 2012), *Cxcl12*-DsRed (Ding and Morrison, 2013), *Ubc-creER* (Ruzankina et al., 2007), *Rosa26-CAG-loxp-stop-loxp-tdTomato* (Madisen et al., 2010), *Rosa26-loxp-stop-loxp-EYFP* (Srinivas et al., 2001), *Rosa26-loxp-stop-loxp-iDTR* (Buch et al., 2005), *NG2-creER*^{TM} (Zhu et al., 2011), *Wnt-1-cre* (Danielian and McMahon, 1996), *Nestin-GFP* (Mignone et al., 2004), *Nestin-creER* (Balordi and Fishell, 2007), *Mx-1-cre* (Kühn et al., 1995), and *Col2.3-GFP* (Kalajzic et al., 2002) mice. To induce CreER activity, male mice (>2-month-old) were injected with 1 mg tamoxifen (Sigma) daily for 5 consecutive days followed by being fed ab libidum with chow containing 400 mg/kg tamoxifen for at least 2 weeks. To induce *Mx-1*-Cre expression, 2-month-old mice were injected with 10 μg poly-inosine:poly-cytosine (pIpC; Amersham)/20 g body mass every other day for 10 days. To treat mice with DT, we injected mice intraperitoneally with 100 ng of DT for 7 consecutive days. All mice were housed in the Animal Resource Center at the University of Texas Southwestern Medical Center (UTSW). All procedures were approved by the UTSW Institutional Animal Care and Use Committee.

For methods related to flow cytometry, bone sectioning, qPCR, culture assay conditions, ossicle formation, irradiation, cell cycle analysis, calcein labeling, micro CT, western analysis, bone fracturing, intrafemoral injection, and subchondral perforation, see the Supplemental Experimental Procedures.

SUPPLEMENTAL INFORMATION

Supplemental Information for this article includes seven figures and Supplemental Experimental Procedures and can be found with this article online at http://dx.doi.org/10.1016/j.stem.2014.06.008.

AUTHOR CONTRIBUTIONS

B.O.Z. performed most of the experiments. R.Y. analyzed the hematopoietic phenotype of *Lepr-cre; Pten*$^{fl/fl}$ mice. M.M.M. obtained most of the 3D images of bone marrow. J.P. analyzed the bone formation rate of *Lepr-cre; iDTR* mice. B.O.Z. and S.J.M. designed and interpreted all experiments and wrote the manuscript.

ACKNOWLEDGMENTS

S.J.M. is a Howard Hughes Medical Institute Investigator, the Mary McDermott Cook Chair in Pediatric Genetics, and the director of the Hamon Laboratory for Stem Cells and Cancer. This work was supported by the National Heart, Lung and Blood Institute (HL097760) and the Cancer Prevention and Research

(F) CFU-Fs per million bone marrow cells.
(G) Percentage of LepR$^+$CD45$^-$Ter119$^-$CD31$^-$ bone marrow stromal cells that incorporated a 14 day pulse of BrdU.
(H–O) MicroCT measurement of cortical (Ct) thickness (H), cortical area (I), total (Tt) area (J), cortical area/total area (Ct.Ar/Tt.Ar) (K), trabecular (Tb) bone volume/total volume (BV/TV) (L), trabecular number (M), trabecular thickness (N), and trabecular spacing (O) of femurs.
(P) Representative microCT images of femurs.
(Q) Representative femur sections showing excessive adipogenesis at metaphyseal bone marrow in *Lepr-cre; Pten*$^{fl/fl}$ mice.
(R) qPCR analysis of transcript levels for genes associated with osteogenic or adipogenic differentiation in LepR$^+$ stromal cells. Transcript levels were normalized based on β-actin amplification then set to 1 in control samples for comparison purposes.
(S) The percentage of CFU-F colonies that contained adipocytes (Oil red O$^+$) and/or osteoblastic cells (Alzarin red S$^+$) after culture in differentiation medium for 3 weeks.
(T) The average number of Perilipin$^+$ adipocytes or Alkaline phosphatase$^+$ (ALP$^+$) osteogenic cells that spontaneously differentiated per CFU-F colony after culture for 1 week in standard medium.
(U) Number of CD150$^+$CD48$^-$Lineage$^-$Sca-1$^+$c-kit$^+$ HSCs in the bone marrow and spleen.
(V) Donor-cell engraftment when 3×10^5 donor bone marrow cells were transplanted along with 3×10^5 recipient bone marrow cells into irradiated recipient mice (n = 11–12 recipient mice per genotype in three experiments).
(W) Frequencies of myeloerythroid-colony-forming progenitors in the bone marrow and spleen.

Institute of Texas. B.O.Z. was supported by a fellowship from the Leukemia and Lymphoma Society. R.Y. was supported by a fellowship from the Damon Runyon Foundation. J.G.P. was supported by a fellowship from the National Science Foundation. We thank Dr. Hung Luu in Children's Medical Center for his expert analysis of hematopoiesis in ossicles and Dr. Aktar Ali in the Mouse Metabolic Phenotyping Core at UT Southwestern for microCT analysis of bone.

Received: February 27, 2014
Revised: May 18, 2014
Accepted: June 6, 2014
Published: June 19, 2014

REFERENCES

Balordi, F., and Fishell, G. (2007). Hedgehog signaling in the subventricular zone is required for both the maintenance of stem cells and the migration of newborn neurons. J. Neurosci. *27*, 5936–5947.

Bianco, P., Robey, P.G., and Simmons, P.J. (2008). Mesenchymal stem cells: revisiting history, concepts, and assays. Cell Stem Cell *2*, 313–319.

Bonaguidi, M.A., Wheeler, M.A., Shapiro, J.S., Stadel, R.P., Sun, G.J., Ming, G.L., and Song, H. (2011). In vivo clonal analysis reveals self-renewing and multipotent adult neural stem cell characteristics. Cell *145*, 1142–1155.

Buch, T., Heppner, F.L., Tertilt, C., Heinen, T.J., Kremer, M., Wunderlich, F.T., Jung, S., and Waisman, A. (2005). A Cre-inducible diphtheria toxin receptor mediates cell lineage ablation after toxin administration. Nat. Methods *2*, 419–426.

Chai, Y., Jiang, X., Ito, Y., Bringas, P., Jr., Han, J., Rowitch, D.H., Soriano, P., McMahon, A.P., and Sucov, H.M. (2000). Fate of the mammalian cranial neural crest during tooth and mandibular morphogenesis. Development *127*, 1671–1679.

Chan, C.K., Chen, C.C., Luppen, C.A., Kim, J.B., DeBoer, A.T., Wei, K., Helms, J.A., Kuo, C.J., Kraft, D.L., and Weissman, I.L. (2009). Endochondral ossification is required for haematopoietic stem-cell niche formation. Nature *457*, 490–494.

Chou, D.B., Sworder, B., Bouladoux, N., Roy, C.N., Uchida, A.M., Grigg, M., Robey, P.G., and Belkaid, Y. (2012). Stromal-derived IL-6 alters the balance of myeloerythroid progenitors during Toxoplasma gondii infection. J. Leukoc. Biol. *92*, 123–131.

Cohen, P., Zhao, C., Cai, X., Montez, J.M., Rohani, S.C., Feinstein, P., Mombaerts, P., and Friedman, J.M. (2001). Selective deletion of leptin receptor in neurons leads to obesity. J. Clin. Invest. *108*, 1113–1121.

Crisan, M., Yap, S., Casteilla, L., Chen, C.W., Corselli, M., Park, T.S., Andriolo, G., Sun, B., Zheng, B., Zhang, L., et al. (2008). A perivascular origin for mesenchymal stem cells in multiple human organs. Cell Stem Cell *3*, 301–313.

Danielian, P.S., and McMahon, A.P. (1996). Engrailed-1 as a target of the Wnt-1 signalling pathway in vertebrate midbrain development. Nature *383*, 332–334.

DeFalco, J., Tomishima, M., Liu, H., Zhao, C., Cai, X., Marth, J.D., Enquist, L., and Friedman, J.M. (2001). Virus-assisted mapping of neural inputs to a feeding center in the hypothalamus. Science *291*, 2608–2613.

Ding, L., and Morrison, S.J. (2013). Haematopoietic stem cells and early lymphoid progenitors occupy distinct bone marrow niches. Nature *495*, 231–235.

Ding, L., Saunders, T.L., Enikolopov, G., and Morrison, S.J. (2012). Endothelial and perivascular cells maintain haematopoietic stem cells. Nature *481*, 457–462.

Echelard, Y., Vassileva, G., and McMahon, A.P. (1994). Cis-acting regulatory sequences governing Wnt-1 expression in the developing mouse CNS. Development *120*, 2213–2224.

Friedenstein, A.J., Chailakhjan, R.K., and Lalykina, K.S. (1970). The development of fibroblast colonies in monolayer cultures of guinea-pig bone marrow and spleen cells. Cell Tissue Kinet. *3*, 393–403.

Fukushi, J., Inatani, M., Yamaguchi, Y., and Stallcup, W.B. (2003). Expression of NG2 proteoglycan during endochondral and intramembranous ossification. Dev. Dyn. *228*, 143–148.

Groszer, M., Erickson, R., Scripture-Adams, D.D., Lesche, R., Trumpp, A., Zack, J.A., Kornblum, H.I., Liu, X., and Wu, H. (2001). Negative regulation of neural stem/progenitor cell proliferation by the Pten tumor suppressor gene in vivo. Science *294*, 2186–2189.

Horwitz, E.M., Le Blanc, K., Dominici, M., Mueller, I., Slaper-Cortenbach, I., Marini, F.C., Deans, R.J., Krause, D.S., and Keating, A.; International Society for Cellular Therapy (2005). Clarification of the nomenclature for MSC: The International Society for Cellular Therapy position statement. Cytotherapy *7*, 393–395.

Joseph, N.M., Mukouyama, Y.S., Mosher, J.T., Jaegle, M., Crone, S.A., Dormand, E.L., Lee, K.F., Meijer, D., Anderson, D.J., and Morrison, S.J. (2004). Neural crest stem cells undergo multilineage differentiation in developing peripheral nerves to generate endoneurial fibroblasts in addition to Schwann cells. Development *131*, 5599–5612.

Kalaitzidis, D., Sykes, S.M., Wang, Z., Punt, N., Tang, Y., Ragu, C., Sinha, A.U., Lane, S.W., Souza, A.L., Clish, C.B., et al. (2012). mTOR complex 1 plays critical roles in hematopoiesis and Pten-loss-evoked leukemogenesis. Cell Stem Cell *11*, 429–439.

Kalajzic, Z., Liu, P., Kalajzic, I., Du, Z., Braut, A., Mina, M., Canalis, E., and Rowe, D.W. (2002). Directing the expression of a green fluorescent protein transgene in differentiated osteoblasts: comparison between rat type I collagen and rat osteocalcin promoters. Bone *31*, 654–660.

Komada, Y., Yamane, T., Kadota, D., Isono, K., Takakura, N., Hayashi, S., and Yamazaki, H. (2012). Origins and properties of dental, thymic, and bone marrow mesenchymal cells and their stem cells. PLoS ONE *7*, e46436.

Komori, T., Yagi, H., Nomura, S., Yamaguchi, A., Sasaki, K., Deguchi, K., Shimizu, Y., Bronson, R.T., Gao, Y.H., Inada, M., et al. (1997). Targeted disruption of Cbfa1 results in a complete lack of bone formation owing to maturational arrest of osteoblasts. Cell *89*, 755–764.

Kühn, R., Schwenk, F., Aguet, M., and Rajewsky, K. (1995). Inducible gene targeting in mice. Science *269*, 1427–1429.

Kunisaki, Y., Bruns, I., Scheiermann, C., Ahmed, J., Pinho, S., Zhang, D., Mizoguchi, T., Wei, Q., Lucas, D., Ito, K., et al. (2013). Arteriolar niches maintain haematopoietic stem cell quiescence. Nature *502*, 637–643.

Lee, J.Y., Nakada, D., Yilmaz, O.H., Tothova, Z., Joseph, N.M., Lim, M.S., Gilliland, D.G., and Morrison, S.J. (2010). mTOR activation induces tumor suppressors that inhibit leukemogenesis and deplete hematopoietic stem cells after Pten deletion. Cell Stem Cell *7*, 593–605.

Liu, Y., Strecker, S., Wang, L., Kronenberg, M.S., Wang, W., Rowe, D.W., and Maye, P. (2013). Osterix-cre labeled progenitor cells contribute to the formation and maintenance of the bone marrow stroma. PLoS ONE *8*, e71318.

Madisen, L., Zwingman, T.A., Sunkin, S.M., Oh, S.W., Zariwala, H.A., Gu, H., Ng, L.L., Palmiter, R.D., Hawrylycz, M.J., Jones, A.R., et al. (2010). A robust and high-throughput Cre reporting and characterization system for the whole mouse brain. Nat. Neurosci. *13*, 133–140.

Maes, C., Kobayashi, T., Selig, M.K., Torrekens, S., Roth, S.I., Mackem, S., Carmeliet, G., and Kronenberg, H.M. (2010). Osteoblast precursors, but not mature osteoblasts, move into developing and fractured bones along with invading blood vessels. Dev. Cell *19*, 329–344.

Magee, J.A., Ikenoue, T., Nakada, D., Lee, J.Y., Guan, K.L., and Morrison, S.J. (2012). Temporal changes in PTEN and mTORC2 regulation of hematopoietic stem cell self-renewal and leukemia suppression. Cell Stem Cell *11*, 415–428.

Méndez-Ferrer, S., Michurina, T.V., Ferraro, F., Mazloom, A.R., Macarthur, B.D., Lira, S.A., Scadden, D.T., Ma'ayan, A., Enikolopov, G.N., and Frenette, P.S. (2010). Mesenchymal and haematopoietic stem cells form a unique bone marrow niche. Nature *466*, 829–834.

Mignone, J.L., Kukekov, V., Chiang, A.S., Steindler, D., and Enikolopov, G. (2004). Neural stem and progenitor cells in nestin-GFP transgenic mice. J. Comp. Neurol. *469*, 311–324.

Morikawa, S., Mabuchi, Y., Kubota, Y., Nagai, Y., Niibe, K., Hiratsu, E., Suzuki, S., Miyauchi-Hara, C., Nagoshi, N., Sunabori, T., et al. (2009). Prospective

identification, isolation, and systemic transplantation of multipotent mesenchymal stem cells in murine bone marrow. J. Exp. Med. *206*, 2483–2496.

Murfee, W.L., Skalak, T.C., and Peirce, S.M. (2005). Differential arterial/venous expression of NG2 proteoglycan in perivascular cells along microvessels: identifying a venule-specific phenotype. Microcirculation *12*, 151–160.

Oguro, H., Ding, L., and Morrison, S.J. (2013). SLAM family markers resolve functionally distinct subpopulations of hematopoietic stem cells and multipotent progenitors. Cell Stem Cell *13*, 102–116.

Omatsu, Y., Sugiyama, T., Kohara, H., Kondoh, G., Fujii, N., Kohno, K., and Nagasawa, T. (2010). The essential functions of adipo-osteogenic progenitors as the hematopoietic stem and progenitor cell niche. Immunity *33*, 387–399.

Otto, F., Thornell, A.P., Crompton, T., Denzel, A., Gilmour, K.C., Rosewell, I.R., Stamp, G.W., Beddington, R.S., Mundlos, S., Olsen, B.R., et al. (1997). Cbfa1, a candidate gene for cleidocranial dysplasia syndrome, is essential for osteoblast differentiation and bone development. Cell *89*, 765–771.

Park, D., Spencer, J.A., Koh, B.I., Kobayashi, T., Fujisaki, J., Clemens, T.L., Lin, C.P., Kronenberg, H.M., and Scadden, D.T. (2012). Endogenous bone marrow MSCs are dynamic, fate-restricted participants in bone maintenance and regeneration. Cell Stem Cell *10*, 259–272.

Pinho, S., Lacombe, J., Hanoun, M., Mizoguchi, T., Bruns, I., Kunisaki, Y., and Frenette, P.S. (2013). PDGFRα and CD51 mark human nestin+ sphere-forming mesenchymal stem cells capable of hematopoietic progenitor cell expansion. J. Exp. Med. *210*, 1351–1367.

Pittenger, M.F., Mackay, A.M., Beck, S.C., Jaiswal, R.K., Douglas, R., Mosca, J.D., Moorman, M.A., Simonetti, D.W., Craig, S., and Marshak, D.R. (1999). Multilineage potential of adult human mesenchymal stem cells. Science *284*, 143–147.

Raghunath, J., Salacinski, H.J., Sales, K.M., Butler, P.E., and Seifalian, A.M. (2005). Advancing cartilage tissue engineering: the application of stem cell technology. Curr. Opin. Biotechnol. *16*, 503–509.

Rivers, L.E., Young, K.M., Rizzi, M., Jamen, F., Psachoulia, K., Wade, A., Kessaris, N., and Richardson, W.D. (2008). PDGFRA/NG2 glia generate myelinating oligodendrocytes and piriform projection neurons in adult mice. Nat. Neurosci. *11*, 1392–1401.

Ruzankina, Y., Pinzon-Guzman, C., Asare, A., Ong, T., Pontano, L., Cotsarelis, G., Zediak, V.P., Velez, M., Bhandoola, A., and Brown, E.J. (2007). Deletion of the developmentally essential gene ATR in adult mice leads to age-related phenotypes and stem cell loss. Cell Stem Cell *1*, 113–126.

Sacchetti, B., Funari, A., Michienzi, S., Di Cesare, S., Piersanti, S., Saggio, I., Tagliafico, E., Ferrari, S., Robey, P.G., Riminucci, M., and Bianco, P. (2007). Self-renewing osteoprogenitors in bone marrow sinusoids can organize a hematopoietic microenvironment. Cell *131*, 324–336.

Schneider, S., Bosse, F., D'Urso, D., Muller, H., Sereda, M.W., Nave, K., Niehaus, A., Kempf, T., Schnolzer, M., and Trotter, J. (2001). The AN2 protein is a novel marker for the Schwann cell lineage expressed by immature and nonmyelinating Schwann cells. J. Neurosci. *21*, 920–933.

Schwab, K.E., and Gargett, C.E. (2007). Co-expression of two perivascular cell markers isolates mesenchymal stem-like cells from human endometrium. Hum. Reprod. *22*, 2903–2911.

Srinivas, S., Watanabe, T., Lin, C.S., William, C.M., Tanabe, Y., Jessell, T.M., and Costantini, F. (2001). Cre reporter strains produced by targeted insertion of EYFP and ECFP into the ROSA26 locus. BMC Dev. Biol. *1*, 4.

Sugiyama, T., Kohara, H., Noda, M., and Nagasawa, T. (2006). Maintenance of the hematopoietic stem cell pool by CXCL12-CXCR4 chemokine signaling in bone marrow stromal cell niches. Immunity *25*, 977–988.

Yilmaz, O.H., Valdez, R., Theisen, B.K., Guo, W., Ferguson, D.O., Wu, H., and Morrison, S.J. (2006). Pten dependence distinguishes haematopoietic stem cells from leukaemia-initiating cells. Nature *441*, 475–482.

Zhang, J., Grindley, J.C., Yin, T., Jayasinghe, S., He, X.C., Ross, J.T., Haug, J.S., Rupp, D., Porter-Westpfahl, K.S., Wiedemann, L.M., et al. (2006). PTEN maintains haematopoietic stem cells and acts in lineage choice and leukaemia prevention. Nature *441*, 518–522.

Zhu, X., Hill, R.A., Dietrich, D., Komitova, M., Suzuki, R., and Nishiyama, A. (2011). Age-dependent fate and lineage restriction of single NG2 cells. Development *138*, 745–753.